

Reactions of Ethyne with Some Ruthenium Cluster Complexes Containing dpmm

by Michael I. Bruce^{*a}), Simon M. Pyke^b), Natasha N. Zaitseva^a), Brian W. Skelton^b), and Allan H. White^b)

^a) Department of Chemistry, University of Adelaide, Adelaide, South Australia 5005
(e-mail: michael.bruce@adelaide.edu.au)

^b) Department of Chemistry, University of Western Australia, Crawley, Western Australia 6009

In memoriam Luigi M. Venanzi, who was an early mentor of the senior author and who first aroused his interest in organometallic chemistry

Reactions of ethyne with $[\text{Ru}_3(\mu\text{-dpmm})(\text{CO})_{10}]$ have given isomeric complexes $[\text{Ru}_3(\mu_3\text{-C}_6\text{H}_6)(\text{CO})_6(\text{dpmm})]$, one of which, **2**, contains the dpmm chelating an Ru-atom, together with a hexatrienetriyl ligand attached to the Ru_3 cluster to form a methylideneruthenacyclohexadiene system. The second isomer **3** contains the dpmm bridging an Ru–Ru bond, with the C_6H_6 ligand forming a vinylruthenacyclopentadiene system. Also isolated was the open-chain Ru_3 complex **4** containing a ruthenacyclopentadiene attached to the central Ru-atom; the other Ru–Ru vector is bridged by a $\text{PPh}_2\text{CHPPh}_2\text{C}_4\text{H}_5$ ligand, formed by a novel insertion of two ethyne molecules into an Ru–P bond. The reaction of ethyne with $[\text{Ru}_3(\mu\text{-H})(\mu_3\text{-C}_2\text{H}_2)(\text{CO})_9]$ proceeded by attack at the coordinated alkyne and at the cluster to give a cluster-bonded $\text{PPh}_2\text{CH}_2\text{PPh}_2\text{CCH}$ system in **7**. Thermolysis of $[\text{Ru}_3(\mu\text{-H})(\mu_3\text{-C}_2\text{SiMe}_3)(\mu\text{-dpmm})(\text{CO})_7]$ (**8**; refluxing MeOH) in the presence of KF gave $[\text{Ru}_6(\mu\text{-CCH}_2)_2(\mu\text{-dpmm})_2(\text{CO})_{12}]$ (**9**; 80%); similar reactions carried out with $[\text{RuClCp}(\text{PPh}_3)_2]$ also present gave **9** (67%) together with $[\text{Ru}_3(\mu\text{-H})(\mu_3\text{-C}_2\text{H})(\mu\text{-dpmm})(\text{CO})_6(\text{PPh}_3)]$ (**11**; 23%). The molecular structures of **2**, **3**, **4**, **7**, **9**, and **11**, some as differently solvated forms, have been determined by single-crystal X-ray studies.

Introduction. – The chemistry of alkynes on metal cluster carbonyls continues to excite interest and is a continuing source of novel structural types [1]. We have recently described some reactions between $[\text{Ru}_3(\text{CO})_{12}]$ and ethyne, which, in addition to such well-known structural types as mono- and binuclear ruthenacyclopentadienes and simple C_2Ru_n ($n=3, 4$) clusters [2], also afforded products of dimerisation reactions, such as $[\text{Ru}_5(\mu_4\text{-CHCHCCH}_2)(\text{CO})_{15}]$, and of disproportionations, such as $[\text{Ru}_6(\mu\text{-H})(\mu_4\text{-C})(\mu_4\text{-CCMe})(\mu\text{-CO})(\text{CO})_{16}]$ [3]. We have also studied the deprotonation and auration of the hydrido-ethynyl complex $[\text{Ru}_3(\mu\text{-H})(\mu_3\text{-C}_2\text{H})(\text{CO})_9]$ [4]. In seeking to extend this work, we have studied both the reactions of ethyne with $[\text{Ru}_3(\mu\text{-dpmm})(\text{CO})_{10}]$ and those between $[\text{Ru}_3(\mu\text{-H})(\mu_3\text{-C}_2\text{H})(\text{CO})_9]$ and dpmm. The former complex has been shown to afford trinuclear complexes of somewhat greater stability than those formed by the parent carbonyl, the products formed by cluster degradation and subsequent build-up being obtained in significantly lower yields [5]. This paper describes some of this chemistry, including novel examples of ethyne trimerisation, as well as of incorporation of the dpmm ligand into new ligands formed on the cluster.

The protodesilylation of trimethylsilyl derivatives of organic compounds with fluoride ion is a useful reaction in organic chemistry [6]. Recently, we have described a modification of the usual synthesis of mononuclear alkynylruthenium complexes by

treating $[\text{RuClCp}(\text{PPh}_3)_2]$ with a variety of trimethylsilylated alkynes and poly-ynes in the presence of KF in MeOH [7]. It is likely that this reaction proceeds with intermediate formation of the corresponding vinylidene, which is deprotonated by the fluoride (or methoxide) base. We were interested to determine whether similar reactions might be applied to cluster-bonded silylated alkynes or alkynyls. This paper also describes the protodesilylation reaction of $[\text{Ru}_3(\mu\text{-H})(\mu_3\text{-C}_2\text{SiMe}_3)(\mu\text{-dppm})(\text{CO})_7]$ [5b], from which an unusual hexanuclear cluster containing vinylidene ligands was isolated.

Results and Discussion. – *Reactions of Ethyne with $[\text{Ru}_3(\mu\text{-dppm})(\text{CO})_{10}]$ (1).* Reactions between $[\text{Ru}_3(\mu\text{-dppm})(\text{CO})_{10}]$ (1) and ethyne were carried out by passing a stream of the gas through a solution of the complex, monitoring the reaction periodically by TLC. The same products were formed either on heating, or from a reaction carried out at room temperature in the presence of Me_3NO . Thus, from a reaction carried out in refluxing THF for 2 h, four complexes were separated by preparative TLC (*Scheme 1*). Elemental analyses and mass spectrometry enabled empirical compositions to be established, while single-crystal X-ray studies were required to determine the precise molecular structures of several of the complexes. Spectroscopic data are collected in *Table 1*, while *Table 2* contains selected structural data.

The first compound to be structurally characterised was $[\text{Ru}_3\{\mu_3\text{-}2\eta^1:\eta^2:\eta^4\text{-}(\text{CH})_4\text{CCH}_2\}(\text{CO})_6(\text{dppm})]$, both unsolvated **2** and subsequently as a benzene sesquisolvate **2s**; *Fig. 1* is a plot of the molecule, from which it can be seen that the dppm ligand chelates one of the Ru-atoms of a closed, almost isosceles triangular cluster (Ru(1)–Ru(2,3) 2.7988, 2.7699(5), Ru(2)–Ru(3) 2.8141(5) Å; Ru(1)–P(1,2) 2.3043(9), 2.375(1) Å (the more precise values found in **2s** are quoted)). A novel trimer of ethyne is attached by all C-atoms to the cluster. The Ru(1)(CH)₆ assembly is best described as a methylenerruthenacyclohexadiene. Atoms Ru(1)C(1–4) form the ruthenacyclohexadiene system (Ru(1)–C(1,5) 2.059(4), 2.096(3) Å) of which atoms C(1–4) bond as an η^4 -diene to Ru(2) (Ru(2)–C(1–4) 2.164–2.299(4) Å), while atoms C(5) and C(6) form an η^2 ligand to Ru(3) (Ru(3)–C(5,6) 2.346, 2.261(3) Å). Separations between adjacent C-atoms are consistent with a partially delocalised diene between C(1) and C(4) and a π -bonded olefin between C(5) and C(6). Atom C(5) has no attached H, while atoms C(1–4) have one each, and atom C(6) has two. The coordination of Ru(1), Ru(2) and Ru(3) is completed by one, two, and three terminal CO ligands, respectively.

The IR spectrum contains only terminal $\tilde{\nu}(\text{CO})$ bands between 2058 and 1915 cm^{-1} , while, in addition to the usual dppm CH_2 and Ph resonances, five well-resolved *multiplet* resonances are found for the C_6H_6 ligand in the $^1\text{H-NMR}$ spectrum. The single protons on C(1,3,4) are found at δ 8.50, 6.21, and 3.82 ppm, respectively, while the signal for H–C(2) lies under the Ph *multiplet* (ca. 7.2). The terminal CH_2 group appears as two *doublets* at δ 1.33 and 3.25 ppm (in both signals the splitting is due to a $^1\text{H}, ^{31}\text{P}$ coupling, the expected geminal $^1\text{H}, ^1\text{H}$ coupling being evident only as a line broadening). Assignments of the ^{13}C resonances follow, with C(1–4) at δ 179.2, 99.1, 103.1, and 77.8, respectively, and C(5,6) at δ 173.5 and 43.9 ppm, respectively. Interestingly, the C-atoms attached to Ru(1) show shielding similar to those in mononuclear metallabenzene complexes, such as $[\text{Ir}(\text{CHCMeCHCMeCH})(\text{PET}_3)_3]$ (δ 167.6) [8]. The

Scheme 1

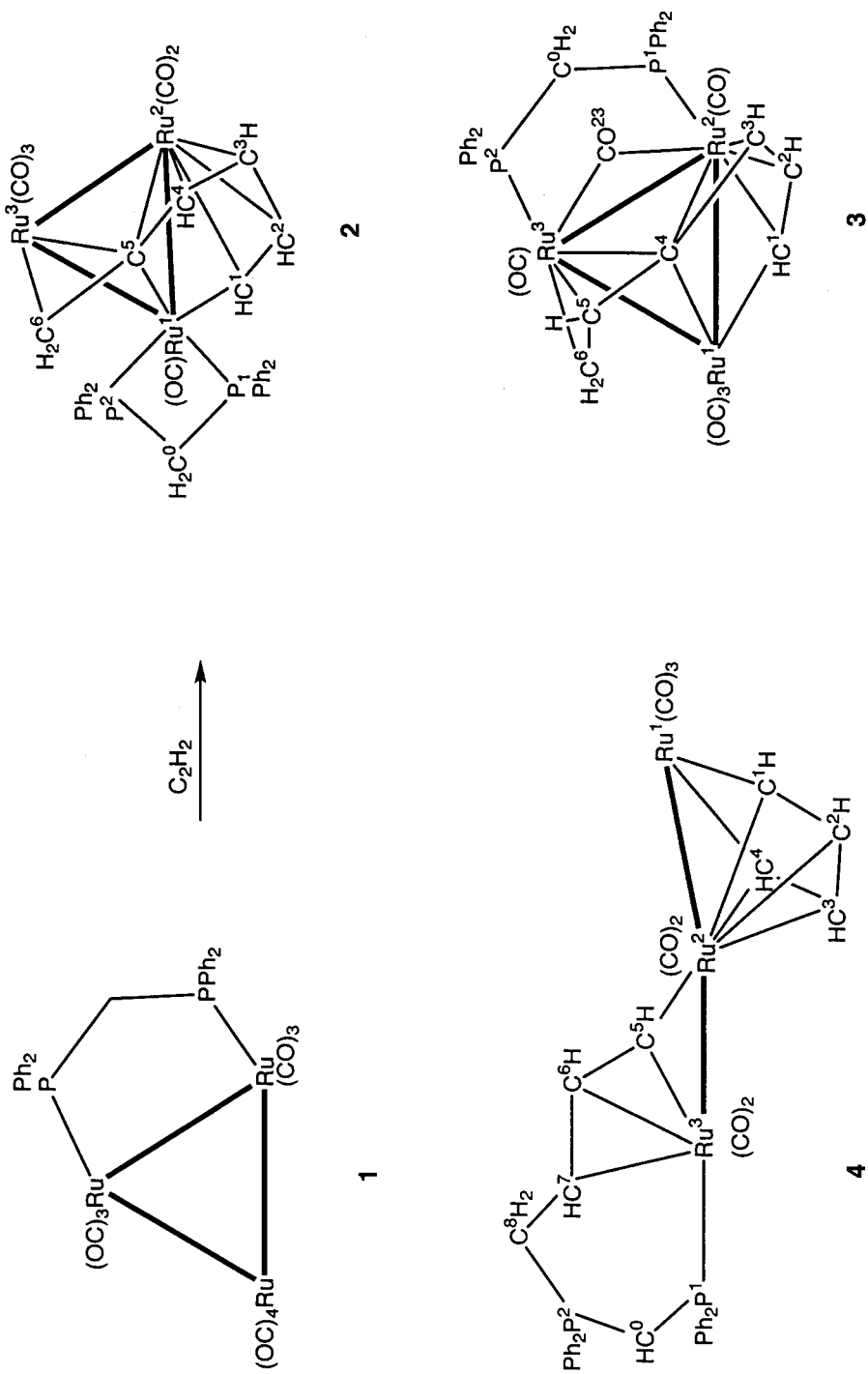


Table 1. Spectroscopic Data for Complexes Described

Complex/analysis	IR ^{a)} $\tilde{\nu}(\text{CO})/\text{cm}^{-1}$	¹ H-NMR ^{b)} δ (J)	MS
[Ru ₃ (μ_3 -2 η^1 : η^2 : η^1 -CH) ₃ CCH ₃](CO) ₆ (dppm)] (2) Calc. for C ₃₇ H ₃₀ O ₆ P ₃ Ru ₃ : C 47.59, H 3.00, M 935; found: C 48.13, H 3.22	2058w, 2040s, 2030m, 2003m, 1991vs, 1976vs, 1949m, 1937w, 1915w	3.30 (<i>d</i> , <i>J</i> (H,H) = 8, 1 CH); 3.87 (<i>d</i> , <i>J</i> (H,H) = 8.5, 1 CH); 4.33 (<i>m</i> , 1 H, CH ₂); 4.59 (<i>m</i> , 1 H, CH ₂); 6.29 (<i>t</i> , <i>J</i> (H,H) = 6, 1 CH); 6.42 (<i>dd</i> , <i>J</i> (H,H) = 11, 2 H, CH ₂); 6.94–8.58 (<i>m</i> , 21 H, Ph + CH)	FAB: 935, (M ⁺), 907–767, ([M–n CO] ⁺) (n = 1–6), 687 ([M–6 CO–Ph] ⁺)
[Ru ₃ (μ_3 -2 η^1 : η^2 : η^1 -CH) ₃ CCH ₃]- (μ -dppm)(μ -CO)(CO)] (3) Calc. for C ₃₇ H ₃₀ O ₆ P ₃ Ru ₃ : C 47.59, H 3.00, M 935; found: C 46.88, H 3.41	2056vs, 2000s, 1978s, 1965s, 1947 (sh), 1885w	1.89 (<i>d</i> , <i>J</i> (H,H) = 10, 1 CH); 2.80 (<i>m</i> , CH ₂); 3.59 (<i>m</i> , 1 CH); 3.77 (<i>m</i> , 1 CH); 4.21 (<i>m</i> , 1 CH); 4.32 (<i>m</i> , 1 CH); 4.92 (<i>d</i> , <i>J</i> (H,H) = 7, 1 CH); 5.81 (<i>m</i> , 1 CH); 6.85–7.44 (<i>m</i> , 24 H, Ph + 2 CH); 7.63 (<i>dd</i> , <i>J</i> (H,H) = 7, CH ₂); 8.05 (<i>d</i> , <i>J</i> (H,H) = 4, 1 CH); 8.11 (<i>d</i> , <i>J</i> (H,H) = 7, CH)	FAB: 935, (M ⁺), 907 ([M–CO] ⁺), 878–766 ([M–H–n CO] ⁺) (n = 2–6)
[Ru ₃ (μ - η^1 : η^2 : η^1 -P-(CH ₂) ₂ PPPh ₂ CHPPPh ₂)- (μ -2 η^1 : η^1 -C ₃ H ₇)(CO)] (4) Calc. for C ₄₀ H ₃₀ O ₃ P ₃ Ru ₃ : C 48.63, H 3.04, M 990; found: C 50.24, H 3.21	2057m, 2022m, 1992s, 1975m, 1968 (sh), 1933vw, 1918w	in (CD ₂) ₂ CO: 2.90, 3.82 (2 <i>m</i> , 1 × 2 H); 4.24, 5.33, 6.16, 6.25, 6.76, 7.10 (6 <i>m</i> , 6 × 1 H); 7.38–8.08 (<i>m</i> , 20 H, Ph)	FAB: 990, (M ⁺), 962–822 ([M–n CO] ⁺) (n = 1–6), 792([M–7 CO–2 H] ⁺)
[Ru ₃ (μ - η^1 : η^2 : η^1 -P-(CH) ₂ (CH ₂) ₂ PPPh ₂ CHPPPh ₂)- (μ -2 η^1 : η^1 -C ₃ H ₇)(CO)(P(OMe) ₃)] (5) Calc. for C ₄₀ H ₃₀ O ₃ P ₃ Ru ₃ : C 48.63, H 3.04, M 990; found: C 50.24, H 3.21	2049s, 2022w, 2005m, 1993 (sh), 1982vs, 1968vs (br), 1962 (sh), 1952m, 1946m		FAB: 1058 ([M–H] ⁺), 1057 ([M–H–CO] ⁺), 1029 ([<i>m</i> –H–2 CO] ⁺), 1000–916 ([<i>m</i> –2 H–n CO] ⁺) (n = 3–6), 789 ([M–5 H–6 CO–P(OMe) ₃] ⁺)
[Ru ₃ (μ -H)(CO) ₆ (dppm)(C ₆ H ₅)] (6)	2066s, 2027m, 2012s, 1993s, 1973 (sh), 1963vs, 1929 (sh)	– 15.21 (<i>t</i> , <i>J</i> (PH) = 12.3, 1 H, RuH); 2.31, 2.57, 2.74 (3 <i>m</i> , 3 × 1 H); 2.91 (<i>d</i> , <i>J</i> (H,H) = 5.4, 1 H); 3.37, 4.34, 4.66, 5.42, 5.56, 6.55 (6 <i>m</i> , 6 × 1 H); 7.04–7.81 (<i>m</i> , Ph); 8.68 (<i>m</i> , 1 H)	FAB: 990 (M ⁺), 971, 944, 907–683 ([M–n CO] ⁺) (n = 1–8)
[Ru ₃ (μ -H)(μ_3 -PPPh ₂ CH ₂ PPPh ₂ CCH)(CO) ₆] (7) Calc. for C ₄₀ H ₃₀ O ₃ P ₃ Ru ₃ : 0.5 CH ₂ Cl ₂ ; C 43.49, H 2.55, M 939; found: C 43.17, H 2.58	2064s, 2012m, 2003vs, 1993s, 1974m, 1958m, 1944w, 1922m	– 19.05 (<i>d</i> , <i>J</i> (H,P) = 6.8, 1 H, RuH); – 18.91 (<i>d</i> , <i>J</i> (H,P) = 6.8, 1 H, RuH); 3.34 (<i>m</i> , 2 CH ₂); 5.32 (<i>s</i> , 1 H, CH ₂ Cl ₂); 6.63–7.95 (<i>m</i> , 40 H, Ph); 8.61 (<i>d</i> , <i>J</i> (H,P) = 2, 1 CH); 8.67 (<i>d</i> , <i>J</i> (H,P) = 2, 1 CH)	FAB: 938 ([M–H] ⁺), 911–714 ([M–H–n CO] ⁺) (n = 1–8), 635 ([M–3 H–8 CO–Ph] ⁺), 558 ([M–3 H–8 CO–2 Ph] ⁺)
[Ru ₃ (μ -CCH ₂)(μ -dppm) ₂ (CO) ₃] (9) Calc. for C ₄₀ H ₃₀ O ₃ P ₃ Ru ₃ : C 44.95, H 2.72, M 1763; 1943w, 1926w, 1910w found: C 44.94, H 2.77	in CH ₂ Cl ₂ : 2023 (sh), 2004vs, 1978s, 1943w, 1926w, 1910w	3.43 (<i>dd</i> , <i>J</i> (H,H) = 4.5, <i>J</i> (H,P) = 15, 1 H, CCH ₂); 3.94 (<i>dt</i> , <i>J</i> (H,H) = 11, <i>J</i> (H,P) = 25, 1 H, PCH ₂); 4.34 (<i>d</i> , <i>J</i> (H,H) = 4.5, 1 H, CCH ₂); 4.57 (<i>dt</i> , <i>J</i> (H,H) = 11, <i>J</i> (H,P) = 24, 1 H, PCH ₂); 6.84–7.73 (<i>m</i> , 20 H, Ph)	ES (MeOH): 1763 (M ⁺), 1735–1651 ([M–n CO] ⁺), (n = 1–4), 1599 ([M–4 CO–2 C ₂ H ₅] ⁺), 1571–1487 ([M–2 C ₂ H ₅ –n CO] ⁺) (n = 5–9)
[Ru ₃ (μ -H)(μ -C ₂ H ₅)(μ -dppm)(CO) ₆ (PPh ₃)] (11) Calc. for C ₃₅ H ₃₀ O ₆ P ₃ Ru ₃ : C 53.54, H 3.41, M 1145; 1945w, 1928m found: C 53.91, H 3.62	2022vs, 1990s, 1977vs, 1961s, 1945w, 1928m	– 19.63 (<i>dd</i> , <i>J</i> (H,H) = 9, <i>J</i> (H,P) = 42, 1 H, RuH); 3.34 (<i>m</i> , 1 H, CH ₂); 4.15 (<i>d</i> , <i>J</i> (H,H) = 9, 1 H, CCH ₂); 4.30 (1 H, CH ₂); 6.17–7.78 (<i>m</i> , 35 H, Ph)	ES (MeOH): 1144 ([M–H] ⁺), 1116 ([M–H–CO] ⁺), 881 ([M–2 H–PPh ₃] ⁺), 853–797 ([M–2 H–PPh ₃ –n CO] ⁺) (n = 1–3)

^{a)} In cyclohexane unless otherwise stated. ^{b)} In CDCl₃ unless otherwise stated.

Table 2. Selected Bond Parameters for **2**, **3**, **4**, **7**, and **11**^{a)}

Complex	2 , 2s	3a , 3b	4 , 4s	7 , 7s	11s
Bond lengths [Å]					
Ru(1)–Ru(2)	2.776(3), 2.7988(5)	2.7265(5), 2.7293(8)	2.714(2), 2.7338(7)	3.032(1), 2.9860(8)	2.817(1)
Ru(1)–Ru(3)	2.764(2), 2.7699(5)	2.8443(7), 2.8389(7)		2.775(1), 2.778(1)	2.805(1)
Ru(2)–Ru(3)	2.809(3), 2.8141(5)	2.7808(5)	2.897(2), 2.8957(7)	2.7587(9), 2.758(1)	2.797(1)
Ru(1)–P(1)	2.297(5), 2.3043(9)			2.322(2), 2.310(2)	2.328(3)
Ru(2)–P(1)		2.3204(9), 2.310(2)			
Ru(3)–P(1)			2.313(3), 2.326(2)		
Ru(3)–P(2)		2.2602(9), 2.263(2)			
Ru(1)–C(1)	2.10(2), 2.059(4)	2.108(4), 2.123(8)	2.04(1), 2.067(7)		2.21(1)
Ru(1)–C(2)				2.085(4), 2.085(8)	2.24(1)
Ru(1)–C(4)		2.112(4), 2.103(8)	2.09(1), 2.070(7)		
Ru(2)–C(1)	2.12(2), 2.164(4)	2.166(4), 2.149(7)	2.22(1), 2.255(7)	2.073(6), 2.07(1)	1.94(1)
Ru(2)–C(2)	2.22(2), 2.258(4)	2.257(5), 2.265(8)	2.24(1), 2.252(7)		
Ru(2)–C(3)	2.25(3), 2.269(4)	2.298(5), 2.298(8)	2.26(1), 2.286(7)		
Ru(2)–C(4)	2.33(3), 2.299(4)	2.485(5), 2.484(8)	2.27(1), 2.288(6)		
Ru(2)–C(5)			2.12(1), 2.101(6)		
Ru(3)–C(1)				2.227(6), 2.230(5)	2.20(1)
Ru(3)–C(2)				2.208(5), 2.213(5)	2.21(1)
Ru(3)–C(4)		2.347(4), 2.330(7)			
Ru(3)–C(5)	2.30(2), 2.346(3)	2.257(5), 2.259(8)	2.12(1), 2.164(6)		
Ru(3)–C(6)	2.28(3), 2.261(3)	2.279(5), 2.280(9)	2.21(1), 2.197(6)		
Ru(3)–C(7)			2.28(1), 2.277(6)		
P(1,2)–C(0)	1.85, 1.85(2); 1.841, 1.859(4)	1.852, 1.836(4); 1.853, 1.839(6)	1.72, 1.66(1); 1.734, 1.687(6)	1.864, 1.803(5); 1.86(1), 1.790(5)	1.83, 1.84(1)
P(2)–C(2)				1.761(6), 1.781(8)	
P(2)–C(8)			1.83(1), 1.807(6)		
C(1)–C(2)	1.35(5), 1.405(6)	1.421(7), 1.43(1)	1.37(2), 1.39(1)	1.371(7), 1.381(8)	1.32(1)
C(2)–C(3)	1.41(5), 1.426(5)	1.397(6), 1.41(1)	1.43(2), 1.43(1)		
C(3)–C(4)	1.45(3), 1.402(6)	1.445(6), 1.44(1)	1.43(2), 1.41(1)		
C(4)–C(5)	1.43(4), 1.439(5)	1.439(6), 1.44(1)			
C(5)–C(6)	1.44(3), 1.413(5)	1.401(6), 1.39(1)	1.41(2), 1.406(9)		
C(6)–C(7)			1.44(2), 1.423(9)		
C(7)–C(8)			1.47(2), 1.515(9)		
Bond angles [deg.]					
Ru(1)–Ru(2)–Ru(3)	59.30(7), 59.14(1)	62.18(1), 62.03(2)	144.72(5), 147.17(2)	57.04(2), 57.67(2)	59.93(3)
Ru(2)–Ru(1)–P(1)	133.8(2), 133.04(3)			148.18, 150.45(7)	89.21(9)
Ru(1)–P(1)–C(0)	96.6(6), 96.4(1)			109.0(2), 109.2(2)	111.6(5)
P(1)–C(0)–P(2)	95(1), 95.1(2)	113.0(2), 113.0(4)	124.9(6), 123.0(4)	110.2(4), 109.7(5)	113.4(6)
C(0)–P(2)–Ru(2)					111.6(4)
C(0)–P(2)–C(2)				105.6(2), 106.0(4)	
P(2)–C(2)–C(1)				124.7(4), 125.9(7)	
Ru(1)–C(1)–C(2)	127(2), 130.0(3)	116.9(3), 117.2(6)	118.0(9), 116.3(5)		74.2(8)
Ru(2)–C(4)–C(3)	69(2), 71.0(2)	65.5(3), 65.5(4)	71.1(7), 71.9(4)		
Ru(2)–C(5)–C(6)			125.0(8), 125.9(4)		
C(1)–Ru(2)–C(4)	84.4(9), 82.8(1)	68.9(2), 69.2(3)	70.7(4), 69.4(2)		
C(1)–C(2)–C(3)	125(2), 121.2(4)	113.3(4), 111.7(7)	114(1), 115.7(6)		
C(2)–C(3)–C(4)	124(3), 124.8(4)	117.9(4), 118.8(7)	115(1), 112.9(7)		
C(3)–C(4)–C(5)	126(3), 129.2(3)	118.2(4), 117.7(7)			
C(4)–C(5)–C(6)	109(2), 113.8(3)	122.7(4), 122.0(7)			
C(5)–C(6)–C(7)			121(1), 122.1(5)		
C(6)–C(7)–C(8)			117(1), 118.4(5)		
C(7)–C(8)–P(2)			115.7(8), 115.5(4)		

^{a)} Additional data: For **2** [**2s**]: Ru(1)–P(2) 2.376(6) [2.375(1)], Ru(1)–C(5) 2.06(3) [2.096(3)] Å, Ru(1)–C(1)–Ru(2) 82.2(6) [83.0(1)], Ru(1)–C(5)–Ru(3) 78.5(8) [76.9(1)]°. For **4** [**4s**]: C(5)–C(6)–C(7) 121(1) [122.1(5)], C(6)–C(7)–C(8) 117(1) [118.4(5)], Ru(2)–Ru(3)–P(1) 162.22(9) [163.83(4)], Ru(3)–P(1)–C(0) 114.2(4) [114.4(2)]°.

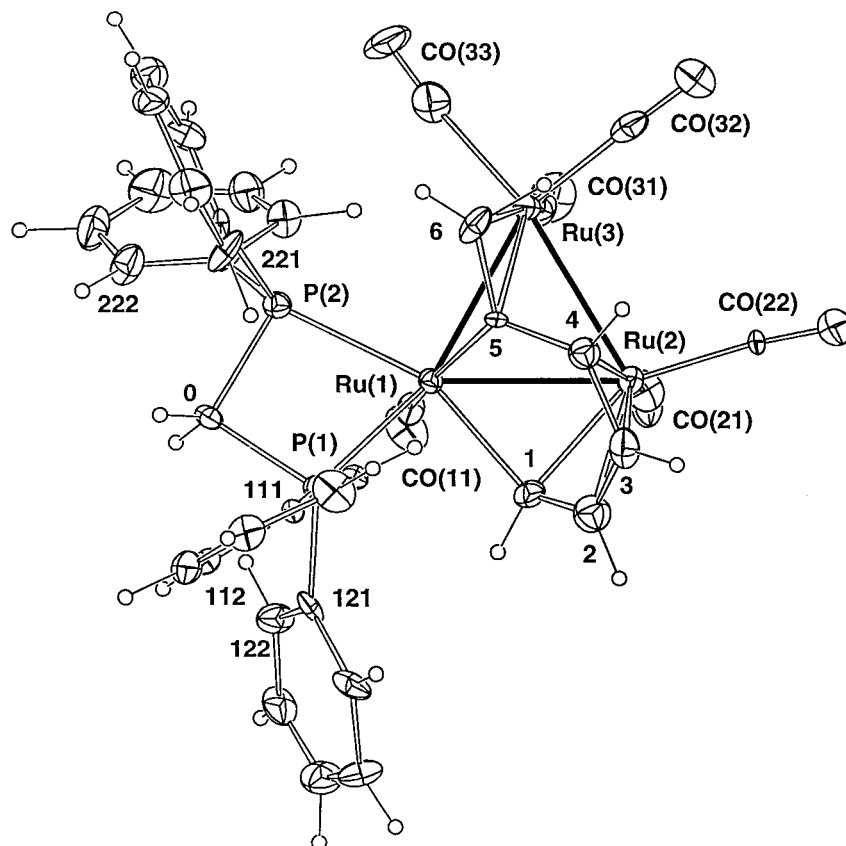


Fig. 1. Projection of a molecule of $[Ru_3(\mu_3\text{-CH})(\mu_3\text{-CHCHCHC=CH}_2)(CO)_6(\text{dppm})]$ (**2s**) showing the atom numbering scheme, C-atoms being denoted by number only

dppm CH_2 group resonates at δ 55.2 ppm. There are low-intensity signals present, which may correspond to a minor isomer in equilibrium, although this has not been established unequivocally.

Complex **3**, which is an isomer of **2**, travelled as two closely spaced bands up the TLC plate and was obtained as isomorphous benzene and toluene monosolvates **3a** and **3b**, respectively, which contained essentially identical molecules of the cluster $Ru_3\{\mu_3\text{-}2\eta^1\text{:}\eta^3\text{:}\eta^4\text{-(CH)}_3\text{CCHCH}_2\}(\mu\text{-dppm})(CO)_6$ (Fig. 2). Atoms Ru(1) and Ru(2) of the closed Ru_3 cluster are bridged by dppm and CO ligands, which results in a relatively long Ru–Ru separation (2.8443(7) Å (values for **3a** given)). Three ethyne molecules have linked to form a second trimer, derived from a hexatriene which is attached to Ru(1) by σ -bonds from C(1) and C(4) (Ru(1)–C(1,4) 2.108, 2.112(4) Å), to Ru(2) by atoms C(1–4) acting as an η^4 -diene (Ru(2)–C(1–4) 2.166–2.485(5) Å) and to Ru(3) by an allylic interaction with atoms C(4–6) (Ru(3)–C(4,5,6) 2.347, 2.257, 2.279(5) Å). Here, we find atom C(4) has no attached H-atom, with one H-atom attached to C(1,2,3,5) and two to C(6). Considerable strain is evident in the

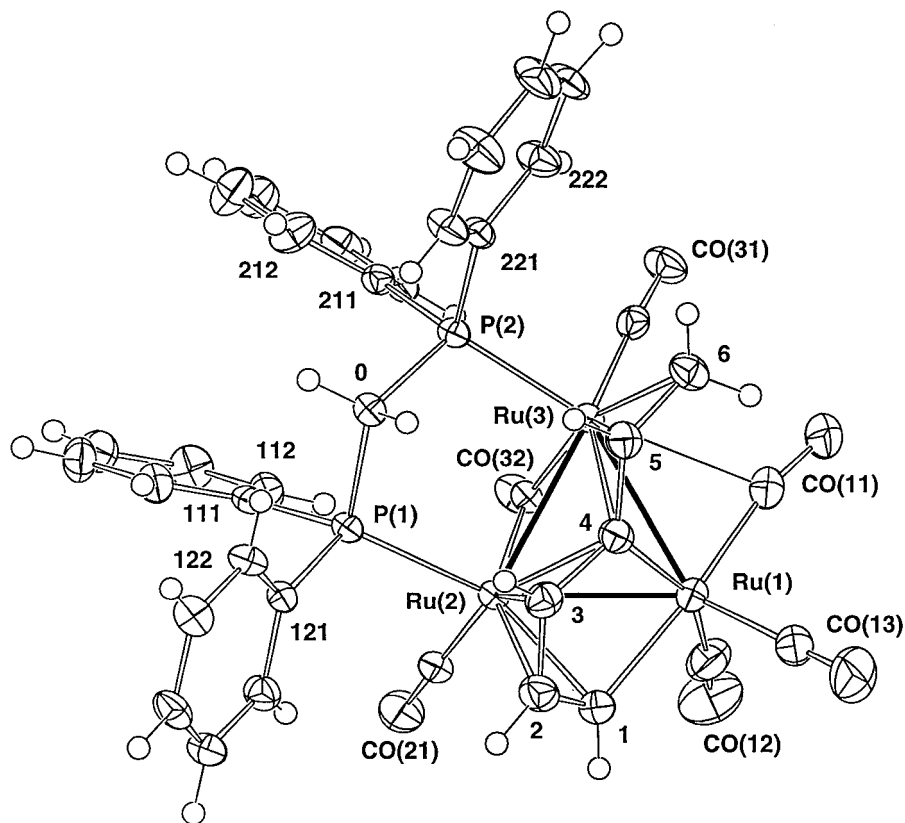


Fig. 2. Plot of a molecule of $[\text{Ru}_3(\mu_3\text{-C}_4\text{H}_3\text{CHCH}_2)(\mu\text{-dppm})(\mu\text{-CO})(\text{CO})_5]$ (**3a**)

coordination of the triene to the cluster, the interaction of the ruthenacyclopentadiene system with the third Ru-atom leading to significantly lengthened Ru(2,3)–C(4) distances.

The IR $\tilde{\nu}(\text{CO})$ spectrum of **3** is simpler than that of **2**, containing only five absorptions in the terminal region between 2056 and 1885 cm^{-1} . The six protons of the C_6H_6 ligand give well-resolved *multiplets* in the NMR spectrum, of which the resonances at δ 8.11, 5.83, and 4.32 ppm have been assigned to protons on C(1,2,3), respectively. The H-atoms of the vinyl group give rise to signals at δ 3.76 (H–C(5)) and at δ 1.89 and 2.86 ppm (H–C(6a) and H–C(6b), resp.). Atoms C(1–4) resonate at δ 160.1, 100.6, 91.4, and 136.9 ppm, respectively, while C(5) (80.5) and C(6) (61.9) are at lower field. The dppm CH_2 carbon is found at δ 47.2 ppm. The mass spectrum contains M^+ at m/z 935, which loses one CO group; subsequent fragmentation involves loss of up to five CO groups from $[M - \text{CO} - \text{H}]^+$.

Complex **4** crystallised in two forms, one solvent-free and the other an isomorphous hexane monosolvate, **4** and **4s**, respectively. In contrast to the first two complexes, the cluster (Fig. 3) contains a bent Ru_3 array (Ru(2)–Ru(1,3) 2.7338, 2.8957(7) Å; Ru(1)–Ru(2)–Ru(3) 147.17(52)° (values for **4s** given)). Two ethyne molecules have

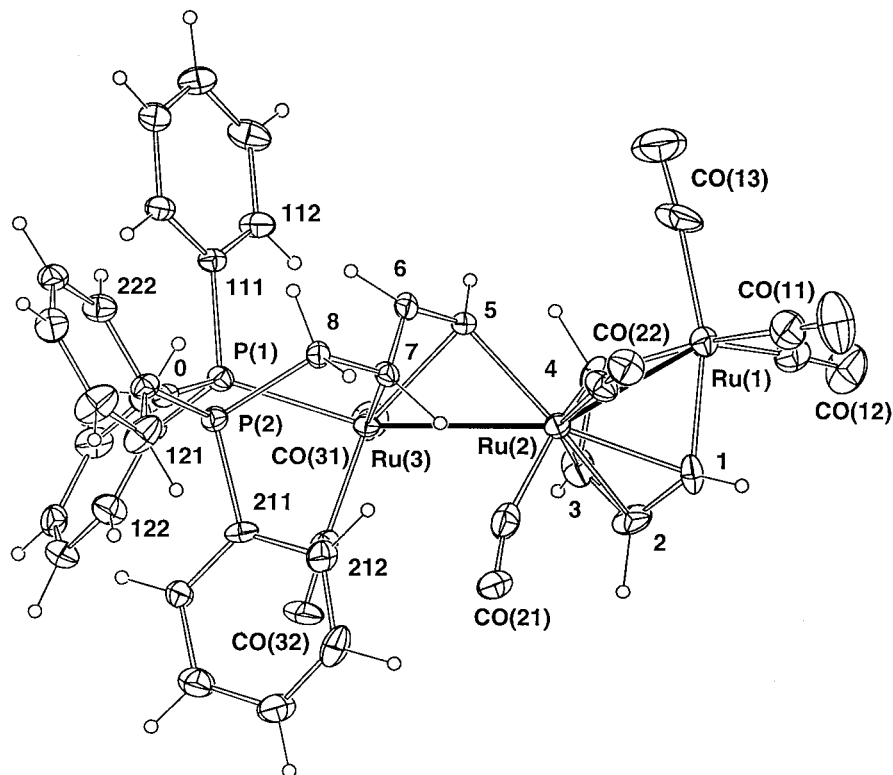


Fig. 3. Plot of a molecule of $[Ru_3(\mu\text{-}PPh_2CHPPh_2CH_2CHCHCH)(\mu\text{-}2\eta^1:\eta^4\text{-}C_4H_4)(CO)_7]$ (**4**)

linked to form a conventional ruthenacyclopentadiene (Ru(1)–C(1,4) 2.067, 2.070(7) Å) which is π -bonded to Ru(2) (Ru(2)–C(1–4) 2.252–2.288(6) Å). The Ru(2)–Ru(3) vector is bridged by the novel $PPh_2CHPPh_2CH_2(CH)_3$ ligand formed by a novel insertion of two molecules of ethyne into the Ru–P(dppm) bond, with concomitant migration of a H-atom from C(0) to C(8). Atom P(1) remains attached to Ru(3) (2.326(2) Å). Atoms C(5–7) form an allylic system coordinated to Ru(3) (Ru(3)–C(5–7) 2.164–2.277(6) Å), of which C(5) is also σ -bonded to Ru(2) (2.101(6) Å).

Only terminal $\tilde{\nu}(CO)$ bands are found in the IR spectrum between 2057 and 1918 cm^{-1} , while the M^+ ion in the mass spectrum at m/z 990 loses up to seven CO ligands. In the 1H -NMR spectrum, *multiplets* at δ 2.00 and 2.73 (H–C(8a) and H–C(8b)), 2.05 (H–CH(7)), 5.08 (H–(6)), 5.91 (H–(2)), 6.06 (H–C(3)), 6.84 (H–C(1)), and 7.74 ppm (H–C(5)) have been assigned; the signal of H–C(4) lies under the Ph *multiplet* (ca. 7.2). The ylidic H–C(0) appears at δ 1.28 ppm. In the ^{13}C -NMR spectrum, C(1–4) are found at δ 143.9, 109.2, 114.3, and 158.8 ppm, respectively, and C(5–8) are found at δ 133.5, 111.6, 55.0, and 29.5 ppm, respectively. The ylidic C(0) resonates at δ 5.8 ppm.

A reaction between **4** and $P(OMe)_3$ afforded the corresponding CO-substitution product **5** in essentially quantitative yield. However, its ready decomposition precluded

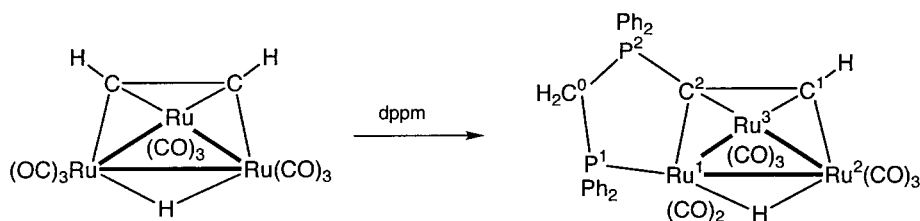
full characterisation of this material. Identification rests on the observation of $[M-H]^+$ at m/z 1085, which fragments by loss of up to five CO groups, followed by the $P(OMe)_3$ ligand.

On account of the instability of the fourth complex, crystals which were satisfactory for an X-ray study could not be obtained. Analytical and spectroscopic data are consistent with the formulation $[Ru_3(\mu-H)(CO)_6(dppm)(C_6H_5)]$ (**6**), but no further characterisation is possible at this stage. The IR spectrum contains five major bands in the terminal $\tilde{\nu}(CO)$ region between 2066 and 1963 cm^{-1} . The 1H -NMR spectrum contains a *triplet* resonance at δ – 15.21 ppm, indicating the presence of a cluster-bonded hydride ligand, together with several *multiplets*, each of relative intensity 1 H, suggesting the presence of an open-chain C_6 ligand. The presence of six CO groups in turn suggests that the organic ligand is a seven-electron donor.

The structures of **2**, **3**, and **4** suggest that a common precursor contains the $Ru_2(CH)_4$ fragment formed by dimerisation of the alkyne on the Ru_3 cluster [2]. Subsequent reactions of the C_4 moiety with a third molecule of ethyne has followed two routes: *i*) insertion of vinylidene, formed by isomerisation of ethyne on the cluster into either an $Ru-C-H$ bond of a so-far unobserved $Ru_3(\mu-C_4H_4)(\mu-dppm)(CO)_8$ intermediate, in part analogous to the known complex $[Ru_3\{\mu_3-C_4(CO_2Me)_4\}(\mu-dppm)(CO)_6]$ [5c], to give the vinylruthenacyclopentadiene **2** or *ii*) into an $Ru-C$ σ -bond of the same intermediate to give **3**. Complex **4** is formed in an unrelated reaction by insertion of C_2H_2 into a $P-Ru$ bond to give the zwitterionic ylide derivative; in this case, the $\mu-C_4H_4$ ligand remains unchanged. Concomitant reactions involve conversion of the bridging dppm ligand to the chelating mode in **3**, and opening of the Ru_3 cluster in **4**.

Reactions of $[Ru_3(\mu_3-C_2H_2)(\mu-CO)(CO)_9]$ with dppm. As an alternative route into Ru cluster complexes containing both ethyne- and dppm-derived ligands, we examined the reaction between $[Ru_3(\mu_3-HC_2H)(\mu-CO)(CO)_9]$ [2a] and dppm. However, the only complex which could be characterised was $[Ru_3(\mu-H)(\mu_3-PPh_2CH_2PPh_2CCH)(CO)_8]$ (**7**; Scheme 2), obtained in moderate yield in unsolvated and CH_2Cl_2 hemisolvate forms, **7** and **7s**, respectively. As shown by the X-ray structural determinations (Fig. 4), the molecule consists of a closed Ru_3 cluster carrying an ylidic ligand formed by attack of the dppm both at the coordinated ethyne and at one Ru-atom of the cluster. The isosceles Ru_3 cluster contains one long $Ru-Ru$ bond ($Ru(1)-Ru(2)$ 2.9860(8) Å (values for **7s** given)), which is bridged by both the hydride and C_2 unit. The organic ligand is bonded to $Ru(1)$ by $P(1)$ (2.310(2) Å) and to all three Ru-atoms by the C_2 unit ($Ru(1)-C(2)$ 2.085(8), $Ru(2)-C(1)$ 2.07(1), $Ru(3)-C(1,2)$ 2.230, 2.213(5) Å).

Scheme 2



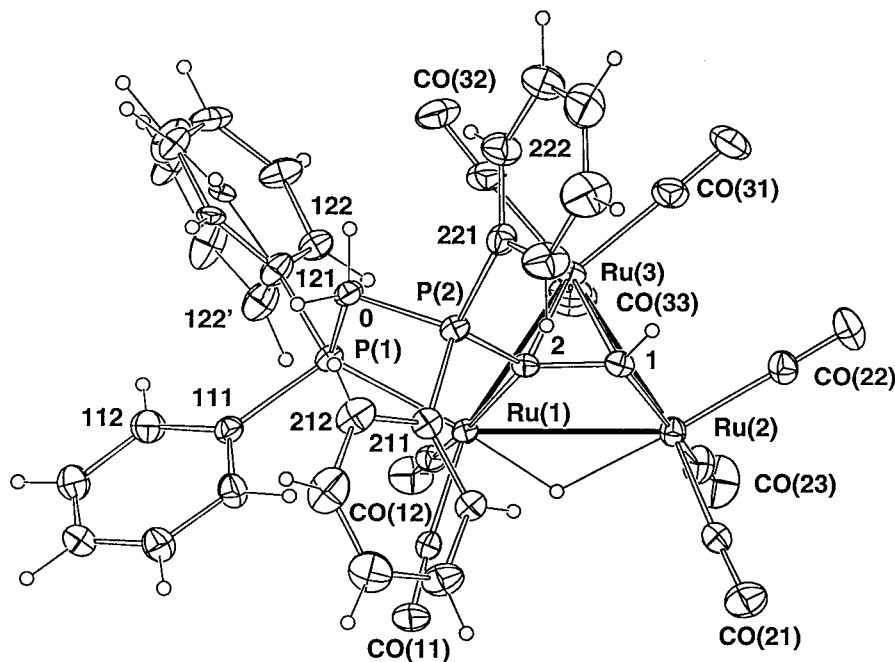


Fig. 4. Plot of a molecule of $[Ru_3(\mu-H)(\mu_3-HC_2PPh_2CH_2PPh_2)(CO)_3]$ (**7s**)

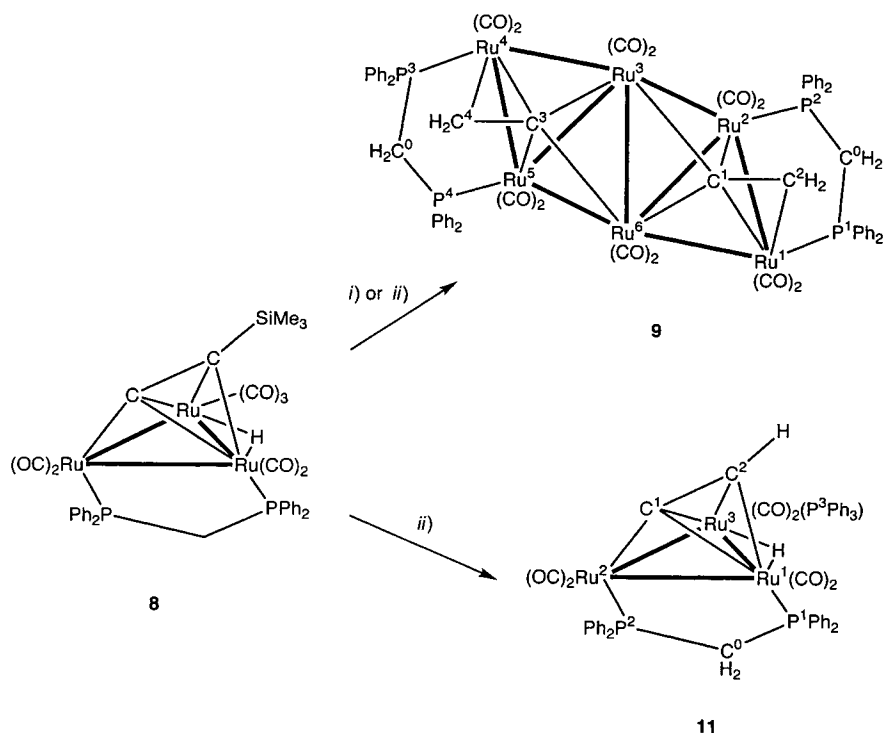
The spectroscopic properties of **7** are consistent with its solid-state structure. The IR spectrum contains an all-terminal $\tilde{\nu}(\text{CO})$ pattern between 2064 and 1922 cm^{-1} , while the $^1\text{H-NMR}$ spectrum contains a high-field *doublet* at $\delta - 19.05$; the H–C(1) appears as a *doublet* at $\delta 8.67$ ppm. The mass spectrum contains a ion centred on m/z 938 corresponding to $[M - H]^+$, which fragments by stepwise loss of up to eight CO groups and one Ph group.

The formation of **7** occurs by simple attack of the dppe on the coordinated ethyne, as found earlier for the reaction between monodentate tertiary phosphines and coordinated alkynes [9]; after P–C bond formation, the second P-atom attacks the cluster with displacement of CO. The resulting complex is formally zwitterionic, the positive P-centre being balanced by a formal negative charge on the Ru_3 cluster.

Protodesilylation Reactions of $[Ru_3(\mu-H)(\mu_3-C_2SiMe_3)(\mu-dppm)(CO)_7]$. Heating the complex $[Ru_3(\mu-H)(\mu_3-C_2SiMe_3)(\mu-dppm)(CO)_7]$ (**8**) in refluxing MeOH in the presence of KF resulted in the formation of a single product in almost quantitative yield. Dark red crystals of $[Ru_6(\mu-CCH_2)_2(\mu-dppm)_2(CO)_{12}]$ (**9**; Scheme 3) were obtained in 80% yield and were initially characterised as the benzene trisolvate, **9s**, on the basis of elemental microanalysis and an electrospray (ES) negative-ion mass spectrum. The molecular anion at m/z 1763 fragmented by loss of CO and C_2H_2 groups. A plot of the molecular structure of **9**, determined from a single-crystal X-ray study, is shown in Fig. 5, important bond parameters being collected in Table 3.

The structure of **9** is based on two edge-fused Ru_4 butterflies, which alternatively can be considered to form a nonplanar triangulated Ru_6 raft. The outer parallel edges

Scheme 3



are bridged by two dppm ligands, while two CCH₂ ligands are held in the clefts of the Ru₄ butterflies. The coordination about each Ru-atom is completed by two terminal CO ligands. The molecule has quasi-two-fold symmetry, the structural parameters being similar in the two halves which are related by a line through the mid-point of the Ru(3)–Ru(6) vector. The Ru–Ru distances range between 2.6918(9) and 2.9764(8) Å, the shortest being the common edge of the two butterflies. The longest pair (2.9764, 2.9647(8) Å) are the hinge bonds Ru(2)–Ru(6) and Ru(3)–Ru(5). The two Ru–Ru bonds bridged by the dppm ligands have intermediate lengths (2.8533, 2.8620(8) Å), while the remaining edges of the butterflies are between 2.7231 and 2.7727(9) Å.

The vinylidene ligands are each attached by C(1) or C(3) to four Ru-atoms. Bonds to the hinge Ru-atoms are shorter than those to the wing-tip Ru-atoms, the lengths for C(1) (2.068, 2.082(8) Å) differing somewhat from those for C(3) (2.099, 2.100(7) Å). Both are consistent with π -type bonding of the C=C units to these metal atoms. The Ru(3)–C(1) and Ru(6)–C(3) bond lengths are 2.168(7) and 2.179(7) Å, respectively. The C–C bond lengths (1.42, 1.38(1) Å) show that some elongation of the formal C=C bonds has occurred upon complexation. Atom pairs C(1)–C(2) and C(3)–C(4) are attached to Ru(1) and Ru(4), respectively, with Ru(1)–C(1) and Ru(4)–C(3) separations (2.164, 2.186(7) Å) being considerably shorter than Ru(1)–C(2) and Ru(4)–C(4) (2.233, 2.223(8) Å). The bond lengths found here are similar to those

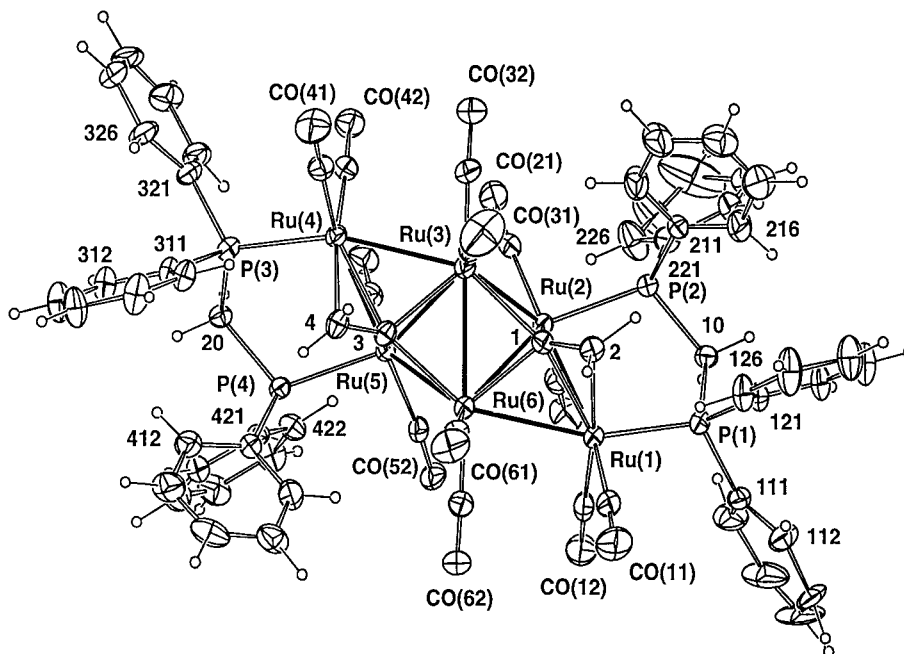


Fig. 5. Projections of a molecule of $[\text{Ru}_6(\mu\text{-CCH}_2)_2(\mu\text{-dppm})_2(\text{CO})_{12}]$ (**9s**) quasi-normal to the putative 2 axis

reported earlier for vinylidene ligands in similar environments, such as those in $[\text{Ru}_4(\mu_3\text{-H})(\mu_4\text{-CCH}^i\text{Pr})(\mu\text{-PPh}_2)(\text{CO})_{10}]$ [8] and $[\text{Ru}_6(\mu_4\text{-S})(\mu_4\text{-CCHCH}=\text{CMe}^i\text{Bu})(\text{CO})_{16}]$ [9].

The spectroscopic properties of **9** are in accord with its solid-state structure. The IR spectrum contains six bands in the terminal $\tilde{\nu}(\text{CO})$ region between 2023 and 1910 cm^{-1} . The $^1\text{H-NMR}$ spectrum contains two *doublets of triplets* at δ 3.94 and 4.57, assigned to the CH_2 protons of the dppm ligands and two *doublets of doublets* at δ 3.43 and 4.34 ppm, assigned to the chemically distinct H-atoms of the two vinylidene groups. The usual Ph *multiplet* is between δ 6.84 and 7.73 ppm.

Complex **9** is closely related to $[\text{Ru}_6(\mu_4\text{-CCH}_2)_2(\text{CO})_{16}]$ (**10**), the latter conforming to ideal 2-symmetry crystallographically. Complex **10** was contained in the mixture of products formed by thermolysis of $[\text{Ru}_3(\mu_3\text{-HC}_2\text{H})(\mu\text{-CO})(\text{CO})_9]$ in hexane (50°, 3 h) [2a]. Some structural data are compared in Table 3. In both Ru_6 clusters, the Ru–Ru bonds shared by the two butterfly portions of the Ru_6 cluster are short (2.6918(9) in **9**, 2.686(1) Å in **10**) and are considered to be Ru=Ru bonds. Long Ru \cdots Ru separations (3.3127(8) in **9**, 3.246(1) Å in **10**) are also present. For both complexes, electron counts on individual Ru-atoms are precise, and, as a whole, these are 88 cluster valence electron systems. The relevance of these structures to those of similar complexes containing $\mu_4\text{-}\eta^2\text{-CO}$ ligands (isoelectronic with CCH_2) has been discussed earlier [2a]. The presence of the dppm ligands results in a less pronounced transfer of electron density and consequently the short and long Ru \cdots Ru separations in **9** are both longer than those present in **10**.

Table 3. Selected Bond Parameters for $[Ru_n(\mu-CCH_2)_2(\mu-dppm)_n(CO)_{16-2n}]$ ($n=2$ for **9s**, 0 for **10**)

	9s	10		9	10
Bond distances [Å]					
Ru(1)–Ru(2)	2.8533(9)	2.838(1)	Ru(3)–Ru(6)	2.6918(9)	2.686(1)
Ru(1)–Ru(6)	2.7727(9)	2.756(1)	Ru(4)–Ru(5)	2.8620(8)	2.838(1)
Ru(2)–Ru(3)	2.7231(9)	2.712(1)	Ru(3)–Ru(4)	2.7702(9)	2.756(1)
Ru(2)⋯Ru(5)	3.3127(8)	3.246(1)	Ru(5)–Ru(6)	2.7278(8)	2.712(1)
Ru(2)–Ru(6)	2.9647(9)	2.943(1)	Ru(3)–Ru(5)	2.9764(8)	2.943(1)
Ru(1)–P(1)	2.301(2)		Ru(4)–P(3)	2.303(2)	
Ru(2)–P(2)	2.314(2)		Ru(5)–P(4)	2.318(2)	
Ru(1)–C(1)	2.164(7)	2.181(6)	Ru(4)–C(3)	2.186(7)	2.181(6)
Ru(1)–C(2)	2.233(8)	2.222(8)	Ru(4)–C(4)	2.223(8)	2.222(8)
Ru(2)–C(1)	2.082(8)	2.069(7)	Ru(5)–C(3)	2.100(7)	2.069(7)
Ru(3)–C(1)	2.168(7)	2.139(6)	Ru(6)–C(3)	2.179(7)	2.139(6)
Ru(6)–C(1)	2.068(7)	2.124(7)	Ru(3)–C(3)	2.099(7)	2.124(7)
C(1)–C(2)	1.42(1)	1.39(1)	C(3)–C(4)	1.38(1)	1.39(1)
Bond angles [deg.]					
Ru(1)–P(1)–C(10)	109.0(2)		Ru(4)–P(3)–C(20)	109.1(2)	
Ru(2)–P(2)–C(10)	113.8(2)		Ru(5)–P(4)–C(20)	113.6(2)	
P(1)–C(10)–P(2)	114.4(4)		P(3)–C(20)–P(4)	115.3(4)	
Interplanar angles					
	9^a	10			
Ru(1,2,6)/Ru(2,3,6)	49.63(4)	50.37(4)			
Ru(2,3,6)/Ru(3,5,6)	81.76(4)	80.67(4) ^b			
Ru(3,5,6)/Ru(3,4,5)	48.82(4)	50.37(4)			

^a) Additional data for **9**: Ru(2)–P(2) 2.294(3), Ru(3)–P(3) 2.334(4) Å, Ru(1)–Ru(3)–P(3) 111.3(1)°. ^b) The value of 46.35(5)° in [2a] is in error, as also is the value of 81.85(4)° for Ru(1,2,3)/Ru(2,2',3'), which should be 72.17(4)°.

We attempted to trap the putative alkynyl cluster by carrying out the reaction in the presence of $[RuCl(PPh_3)_2Cp]$ which, as described above, is susceptible to alkynylation reactions under the conditions used for the synthesis of **9**. Two products were isolated from this reaction, identified as **9**, obtained in 67% yield, and the yellow PPh_3 -substituted protodesilylated starting complex $[Ru_3(\mu-H)(\mu_3-C_2H)(\mu-dppm)(CO)_6(P-Ph_3)]$ (**11**), in 23% yield, characterised by an X-ray crystal-structure determination of its benzene monosolvate **11s**.

A projection of a molecule of **11** is shown in *Fig. 6* with selected bond parameters given in *Table 2*. The structure is similar to that of $[Ru_3(\mu-H)(\mu_3-C_2Ph)(\mu-dppm)(CO)_7]$, with an Ru_3 core supporting the ethynyl group in the common $2\sigma,\pi$ mode: C(1) is σ -bonded to Ru(2) and both C-atoms are π -bonded to atoms Ru(1) and Ru(3). The dppm ligand bridges the Ru(1)–Ru(2) vector (2.817(1) Å), while the PPh_3 ligand occupies an equatorial position on Ru(3). The Ru(1)–Ru(3) separation (2.805(1) Å) is bridged by the alkyne (\perp) and the hydride (which, like the H–C(2), was not located in the structure determination). Structural parameters are similar to those found in related complexes, such as $[Ru_3(\mu-H)(\mu_3-C_2^tBu)(\mu-dppm)(CO)_7]$ [11] and $[Ru_3(\mu-dppm)(CO)_9\{PPh_2(C_6H_4CHO-2)\}]$ [12].

Spectroscopic data are consistent with the solid-state structure being preserved in solution. The $\tilde{\nu}(CO)$ spectrum contains terminal CO bands between 2022 and

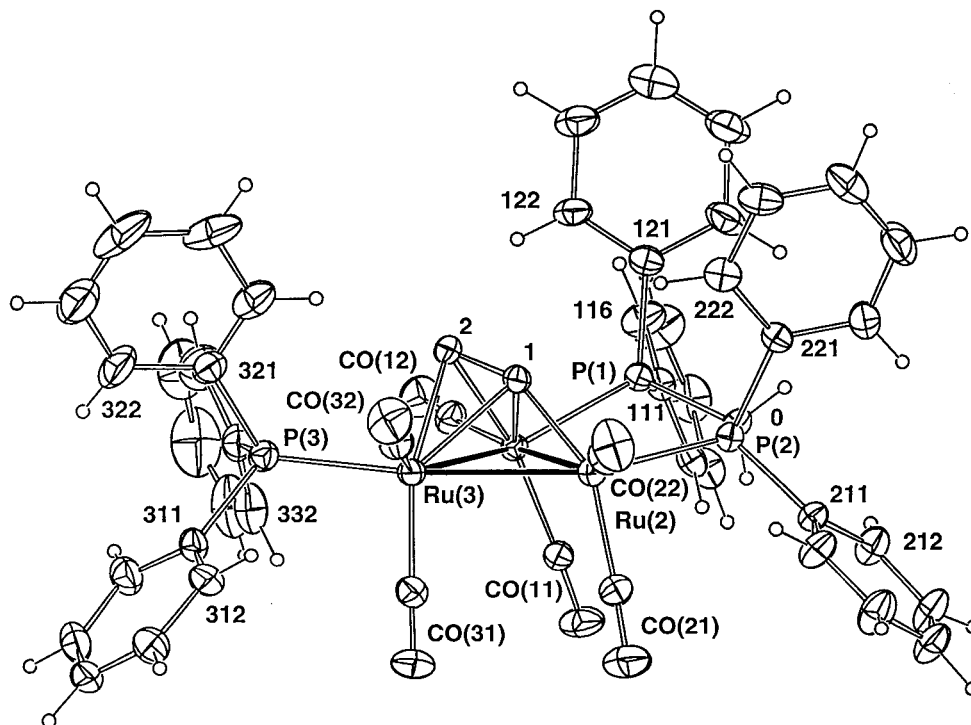


Fig. 6. Plot of a molecule of $[[\text{Ru}_3(\mu\text{-H})(\mu_3\text{C}_2\text{H})(\mu\text{-dppm})(\text{CO})_6(\text{PPh}_3)]]$ (**11s**). The core H-atom, not locatable in the X-ray study, is omitted

1928 cm^{-1} , while the $^1\text{H-NMR}$ spectrum contains a *doublet of doublets* at $\delta -19.63$, assigned to the metal-bonded proton, which is coupled to nonequivalent ^{31}P nuclei, together with a *doublet* resonance at $\delta 4.30$ ppm for the ethynyl proton. Other resonances at $\delta 3.34$ and 4.30 (*multiplets*, dppm) and between $\delta 6.17$ and 7.78 ppm (*multiplet*, Ph) are also present. The highest ion in the negative ES mass spectrum at $m/z 1144$ corresponds to $[\text{M} - \text{H}]^-$ and fragment ions formed by loss of CO and PPh_3 ligands are present.

Discussion. – The various complexes that we have isolated from a series of reactions of ethyne with $[\text{Ru}_3(\mu\text{-dppm})(\text{CO})_{10}]$ or the reverse thereof, and the protodesilylation of $[\text{Ru}_3(\mu\text{-H})(\mu_3\text{-C}_2\text{SiMe}_3)(\mu\text{-dppm})(\text{CO})_7]$, have given further insight into modes of reaction of terminal alkynes with polymetallic systems. Formation of **2**, **3**, and **4** can be envisaged as proceeding through the well-known dimerisation of alkynes on a cluster to give the ruthenacyclopentadiene. This species, which contains a $\text{CH}=\text{CHCH}=\text{CH}$ unit attached to one Ru-atom by two σ bonds and to a second Ru-atom *via* the π system in η^4 mode, was found in **4** and related (substituted) complexes have been described in many earlier reports of the reactions of alkynes with triruthenium-carbonyl clusters. In the present case, further reaction of a third molecule of ethyne may proceed by initial coordination to the third Ru-atom as either an $\eta^2\text{-HCCH}$ (ethyne) or, after isomer-

isation, as an η^1 -CCH₂ (vinylidene) species [13]. Subsequent insertion of these species into an Ru–C σ bond or into a terminal C–H bond of the diene fragment would produce **2** and **3**, respectively.

Further reaction to give complex **4** occurs by cleavage of one Ru–Ru bond, perhaps by a concomitant attack of the dppm ligand on the incoming ethyne. This type of reaction is found in the reaction of [Ru₃(μ_3 -C₂H₂)(μ -CO)(CO)₉] with dppm, which proceeds by nucleophilic attack of the P-atom at an electron-deficient C-atom of the coordinated ethyne and chelation of the second P-atom to the cluster. These reactions were first described many years ago in studies of reactions of monodentate tertiary phosphines with various alkyne–ruthenium and alkyne–osmium clusters [14].

Several reactions are involved in the formation of complex **7**. Formation of a C–P bond may occur, either by direct attack of the incoming ethyne, or after dimerisation at the Ru(2)–Ru(3) centre, on coordinated dppm, possibly after displacement of one arm from the cluster. In this case, we also find migration of one H-atom from the dppm-CH₂ group to atom C(8).

The likely reaction course leading to the formation of the Ru₆ cluster **9** consists of protodesilylation of the μ_3 -C₂SiMe₃ ligand to give the parent ethynyl group [6]. Migration of the cluster-bonded hydride to the ethynyl group to form the vinylidene ligand occurs with concomitant generation of a vacant coordination site which facilitates the coupling of the two Ru₃ cores. The high selectivity of this reaction is notable. This reaction is without precedent, although related reactions leading to coupling of alkynyl groups have been described for [Ru₂(μ -PPh₂)(μ -C₂Bu)(CO)₆] [15], while the structurally similar **10** is formed by thermolysis of [Ru₃(μ_3 -C₂H₂)(μ -CO)(CO)₉] [2a].

Conclusions. – Facile reactions between [Ru₃(μ -dppm)(CO)₁₀] and ethyne have given complexes containing novel oligomers of this alkyne. Formation of the familiar [Ru₂(μ -2 η^1 , η^4 -C₄H₄)] system is followed by further coordination of ethyne, probably to the third Ru-atom. This may isomerise to the vinylidene: insertion of either CCH₂ or HCCH into a C–H bond of the diene affords the observed products **2** or **3**, respectively. An alternative reaction pathway involves cleavage of one Ru–Ru bond, displacement of one dppm-P-atom and intramolecular reaction of the latter with another ethyne dimer. This is accompanied by H-migration from the dppm CH₂ group to the ylidic C-atom of the dppm-C₄H₄ adduct.

Thermolysis of [Ru₃(μ -H)(μ_3 -C₂SiMe₃)(μ -dppm)(CO)₇] in the presence of KF has resulted in protodesilylation and dimerisation accompanied by migration of the cluster-bound hydride to the ethynyl group, generating a vinylidene ligand. This course of reaction is also suggested when the reaction is run in the presence of [RuCl(PPh₃)₂Cp], from which PPh₃ is abstracted to give **11**. The regioselectivity of the first reaction is notable.

Experimental Part

General. The compounds [Ru₃(μ -dppm)(CO)₁₀] [16], [Ru₃(μ_3 -HC₂H)(μ -CO)(CO)₉] [2a] and [Ru₃(μ -H)(μ_3 -C₂SiMe₃)(μ -dppm)(CO)₇] [5b] were prepared by the cited methods. All reactions were carried out under dry, high-purity N₂ by standard *Schlenk* techniques. Solvents were dried, distilled and degassed before use. Prep. TLC was carried out on glass plates (20 × 20 cm) coated with silica (*Merck 60 GF₂₅₄*, 0.5-mm thick). IR: *Perkin-Elmer FT-IR 1920X*; spectra of solns. in cyclohexane (unless otherwise stated) were obtained with a soln. cell-

fitted with NaCl windows (path length 0.5 mm); nujol-mull spectra were collected from samples mounted between NaCl discs. NMR: Samples were dissolved in CDCl_3 (Aldrich, unless otherwise stated) with 5-mm sample tubes; spectra were recorded with Varian Gemini 2000 (^1H : 199.98, ^{13}C : 50.29 MHz) or Varian INOVA (^1H : 599.88, ^{13}C : 150.85 MHz) instruments; assignments of the various resonances of **2**, **3**, and **4** were enabled by COSY, HMBC and HMQC experiments. FAB-MS: VG ZAB 2 HF instrument, with 3-nitrobenzyl alcohol as matrix, Ar as exciting gas, FAB gun voltage 7.5 kV, current 1 mA, accelerating potential 7 kV. ES-MS: samples dissolved in MeOH directly infused into a Finnigan LCQ spectrometer; N_2 as drying and nebulising gas. Elemental analyses were by the Canadian Microanalytical Service, Delta, B.C.

Reactions between Ethyne and $[\text{Ru}_3(\mu\text{-dppm})(\text{CO})_{10}]$. A stream of ethyne was passed through a soln. of $[\text{Ru}_3(\mu\text{-dppm})(\text{CO})_{10}]$ (250 mg, 0.26 mmol) in refluxing THF (30 ml) for 2 h, after which time no starting complex was present (TLC). After removal of solvent, the residue was dissolved in CH_2Cl_2 and separated by prep. TLC (acetone/hexane 3:7) to give five coloured bands and a brown baseline, which was not further examined.

Band 1 (R_f 0.41) contained $[\text{Ru}_3(\mu_3\text{-CH})\{\mu_3\text{-}2\eta^1:\eta^2:\eta^4\text{-}(\text{CH})_4\text{CCH}_2\}(\text{CO})_6(\text{dppm})]$ (**2**; 40 mg, 17%). Red crystals ($\text{C}_6\text{H}_6/\text{pentane}$). Dec. ca. 286° . IR (cyclohexane): see Table 1. $^1\text{H-NMR}$: 1.33 (*d*, $J(\text{P,H}) = 2.4$, 1 H, H-C(6a)); 3.25 (*d*, $J(\text{P,H}) = 8.4$, 1 H, H-C(6b)); 3.82 (*d*, $J(\text{H,H}) = 8.4$, 1 H, H-C(4)); 4.22 (*ddd*, $J(\text{H,H}) = 15.0$, $J(\text{P,H}) = 8.4$, 10.8, 1 H, H-C(0a)); 4.48 (*ddd*, $J(\text{H,H}) = 15.0$, $J(\text{P,H}) = 7.8$, 11.4, 1 H, H-C(0b)); 6.21 (*ddd*, $J(\text{H,H}) = 1.2$, 7.2, 8.4, 1 H, H-C(3)); 6.36–7.63 (*m*, 21 H, H-C(2), arom. H); 8.50 (*ddt*, $J(\text{H,H}) = 1.2$, 7.2, $J(\text{P,H}) = 1.2$, 8.4, 1 H, H-C(1)). $^{13}\text{C-NMR}$: 43.9 (*d*, $J(\text{C,P}) = 9.9$, C(6)); 55.2 (*dd*, $J(\text{C,P}) = 20.8$, 24.3, C(0)); 77.8 (C(4)); 99.1 (C(2)); 103.1 (C(3)); 128.0–138.6 (24 arom. C); 173.5 (*dd*, $J(\text{C,P}) = 6.3$, 10.8, C(5)); 179.2 (*dd*, $J(\text{C,P}) = 11.2$, 30.0, C(1)); 192.8–205.5 (6 C=O). FAB-MS: see Table 1. Analysis: see Table 1.

Band 2 (R_f 0.37) contained $[\text{Ru}_3\{\mu_3\text{-}2\eta^1:\eta^3:\eta^4\text{-}(\text{CH})_3\text{CCHCH}_2\}(\mu\text{-dppm})(\mu\text{-CO})(\text{CO})_5]$ (**3a**; 30 mg, 13%). Dark red crystals ($\text{C}_6\text{H}_6/\text{pentane}$). Dec. $247\text{--}249^\circ$. IR: see Table 1. $^1\text{H-NMR}$: 1.89 (*dt*, $J(\text{H,H}) = 1.8$, 10.8, $J(\text{P,H}) = 1.8$, 1 H, H-C(6a)); 2.79 (*dt*, $J(\text{H,H}) = 11.4$, $J(\text{P,H}) = 10.8$, 1 H, H-C(0a)); 2.86 (*dd*, $J(\text{H,H}) = 1.8$, 6.0, 1 H, H-C(6b)); 3.60 (*dt*, $J(\text{H,H}) = 11.4$, $J(\text{P,H}) = 12.6$, 1 H, H-C(0b)); 3.76 (*ddd*, $J(\text{H,H}) = 6.0$, 10.8, $J(\text{P,H}) = 7.2$, 1 H, H-C(5)); 4.32 (*ddd*, $J(\text{H,H}) = 2.4$, 3.6, $J(\text{P,H}) = 7.2$, 1 H, H-C(3)); 5.83 (*dt*, $J(\text{H,H}) = 3.6$, 5.4, $J(\text{P,H}) = 3.6$, 1 H, H-C(2)); 6.84–7.65 (*m*, 20 arom. H); 8.11 (*dd*, $J(\text{H,H}) = 2.4$, 5.4, 1 H, H-C(1)). $^{13}\text{C-NMR}$: 47.2 (*dd*, $J(\text{C,P}) = 19.8$, 24.5, C(0)); 61.9 (C(6)); 80.5 (C(5)); 91.4 (C(3)); 100.7 (C(2)); 128.1–137.8 (24 arom. C); 136.9 (C(4)); 160.1 (C(1)); 194.0–207.2 (6 C=O). FAB-MS: see Table 1. Analysis: see Table 1.

Band 3 (R_f 0.36) was pink-purple and contained complex **3b** (9 mg) as red crystals (PhMe). The IR and MS data were identical to those of **3a**.

Band 4 (R_f 0.32) afforded small dark purple crystals tentatively formulated as $[\text{Ru}_3(\mu\text{-H})(\mu\text{-dppm})(\text{CO})_8(\text{C}_6\text{H}_5)]$ (**6**, 20 mg). This compound is very unstable in solution. IR: see Table 1. $^1\text{H-NMR}$: see Table 1. FAB-MS: see Table 1.

A broad yellow band (R_f 0.14) contained $[\text{Ru}_3\{\mu\text{-}\eta^1:\eta^2\text{-}P\text{-}(\text{CH})_3\text{CH}_2\text{PPh}_2\text{CHPPPh}_2\}(\mu\text{-}2\eta^1,\eta^4\text{-}C_4H_4)(\text{CO})_7]$ (**4**; 80 mg, 31%). Light yellow solid. M.p. 176° . Dec. 218° . $^1\text{H-NMR}$ (C_6D_6): 1.28 (*dd*, $J(\text{P,H}) = 5.4$, 10.2, 1 H, H-C(0)); 2.00 (*ddd*, $J(\text{H,H}) = 5.4$, 15.0, $J(\text{P,H}) = 28.2$, 1 H, H-C(8a)); 2.05 (*m*, 1 H, H-C(7)); 2.73 (*ddd*, $J(\text{H,H}) = 7.8$, 15.0, $J(\text{P,H}) = 12.0$, 1 H, H-C(8b)); 5.08 (*ddt*, $J(\text{H,H}) = 7.2$, $J(\text{P,H}) = 1.2$, 10.8, 1 H, H-C(6)); 5.91 (*dt*, $J(\text{H,H}) = 2.4$, 6.0, 1 H, H-C(2)); 6.06 (*dd*, $J(\text{H,H}) = 2.4$, 6.0, 1 H, H-C(3)); 6.84 ($J(\text{H,H}) = 2.4$, 6.0, 1 H, H-C(1)); 6.89–7.64 (*m*, 19 H, H-C(4), arom. H); 7.74 (*d*, $J(\text{H,H}) = 7.2$, 1 H, H-C(5)); 7.76 (*m*, 2 H, arom. H). $^{13}\text{C-NMR}$ (C_6D_6): 5.8 (*dd*, $J(\text{C,P}) = 67.8$, 123.5, C(0)); 29.5 (*d*, $J(\text{C,P}) = 22.0$, C(8)); 55.0 (C(7)); 109.2 (C(2)); 111.6 (C(6)); 114.3 (C(3)); 128.5–132.7 (20 \times arom. C); 133.6 (C(5)); 141.5 (arom. C); 141.9 (arom. C); 143.7 (arom. C); 143.9 (C(1)); 144.1 (arom. C); 158.8 (C(4)); 197.2–208.7 [7 C=O]. FAB-MS: see Table 1. Analysis: see Table 1.

A similar reaction was carried out by adding Me_3NO (40 mg, 0.52 mmol) to a soln. containing $[\text{Ru}_3(\mu\text{-dppm})(\text{CO})_{10}]$ (250 mg, 0.26 mmol) in THF (30 ml), which had previously been saturated with ethyne, after which ethyne was passed through the soln. for 2 h at r.t. After removal of solvent and separation of a CH_2Cl_2 extract of the residue by prep. TLC as described above, unreacted $[\text{Ru}_3(\mu\text{-dppm})(\text{CO})_{10}]$ (40 mg, 16%) and complexes **2** (22 mg, 9%), **3** (31 mg, 13%), **4** (110 mg, 43%), and **5** (17.5 mg, 7%) were isolated.

Reaction of Complex 4 with $P(\text{OMe})_3$. A soln. of **4** (65 mg, 0.07 mmol) and $P(\text{OMe})_3$ (12 mg, 0.10 mmol) in thf (5 ml) was stirred at r.t. for 10 min, then Me_3NO (6 mg, 0.08 mmol) was added. After stirring for a further 2 h, complex **3** was no longer present. Evaporation of volatiles under reduced pressure afforded directly $[\text{Ru}_3\{\mu\text{-}\eta^1:\eta^2\text{-}P\text{-}(\text{CH})_3\text{CH}_2\text{PPh}_2\}(\mu\text{-}2\eta^1,\eta^4\text{-}C_4H_4)(\text{CO})_6P(\text{OMe})_3]$ (**5**; 69 mg, 98%). Dec. $154\text{--}156^\circ$. IR: see Table 1. FAB-MS: see Table 1. This complex could not be fully characterised as a result of its ready decomposition.

Reaction between $\text{Ru}_3(\mu_3\text{-HC}_2\text{H})(\mu\text{-CO})(\text{CO})_9$ with dppm. A soln. of Me_3NO (19 mg, 0.246 mmol) in THF (5 ml) was added dropwise to a mixture of $[\text{Ru}_3(\mu_3\text{-HC}_2\text{H})(\mu\text{-CO})(\text{CO})_9]$ (50 mg, 0.082 mmol) and dppm

(64 mg, 0.164 mmol) in the same solvent (15 ml) at r.t. The orange soln. immediately became red. After 30 min, no starting material was present. After removal of THF, the residue was dissolved in CH_2Cl_2 and separated by prep. TLC (acetone/hexane 3:7) into two major fractions.

The first yellow band (R_f 0.28) contained $[\text{Ru}_3(\mu\text{-H})(\mu_3\text{-PPh}_2\text{CH}_2\text{PPh}_2\text{CCH})(\text{CO})_8]$ (**7a**; 30 mg, 39%). Yellow crystals (CH_2Cl_2 /pentane). Dec. 195–197°. $^1\text{H-NMR}$: see *Table 1*. FAB-MS: see *Table 1*. Analysis: see *Table 1*.

The orange band (R_f 0.25) contained $[\text{Ru}_3(\mu\text{-H})(\mu_3\text{-PPh}_2\text{CH}_2\text{PPh}_2\text{CCH})(\text{CO})_8]$ (**7b**; 23 mg, 30%). Orange crystals (CH_2Cl_2 /pentane). The IR and MS data were identical to those of **7a**.

*Preparation of $[\text{Ru}_6(\mu\text{-CCH}_2)_2(\mu\text{-dppm})_2(\text{CO})_{12}$ (**9**)*. A mixture of $[\text{Ru}_3(\mu\text{-H})(\mu_3\text{-C}_2\text{SiMe}_3)(\mu\text{-dppm})(\text{CO})_7]$ (55 mg, 0.056 mmol) and KF (10 mg, 0.16 mmol) was heated in refluxing MeOH (20 ml) for 3 h, then the colour had changed from yellow to red-brown. After removal of solvent, the residue was dissolved in CH_2Cl_2 and separated by prep. TLC (silica gel; acetone/hexane 3:7). A dark brown band (R_f 0.25) was extracted (CH_2Cl_2) and crystallized (benzene/pentane) to give dark red $[\text{Ru}_6(\mu\text{-CCH}_2)_2(\mu\text{-dppm})_2(\text{CO})_{12}]$ (**9**; 39 mg, 80%). IR (CH_2Cl_2): see *Table 1*. $^1\text{H-NMR}$: see *Table 1*. ES-MS: see *Table 1*. Analysis: see *Table 1*.

Reaction of $[\text{Ru}_3(\mu\text{-H})(\mu_3\text{-C}_2\text{SiMe}_3)(\mu\text{-dppm})(\text{CO})_7]$ with $[\text{RuCl}(\text{PPh}_3)_2\text{Cp}]$. A suspension of $[\text{Ru}_3(\mu\text{-H})(\mu_3\text{-C}_2\text{SiMe}_3)(\mu\text{-dppm})(\text{CO})_7]$ (55 mg, 0.056 mmol), $[\text{RuCl}(\text{PPh}_3)_2\text{Cp}]$ (41 mg, 0.056 mmol) and KF (10 mg, 0.16 mmol) was heated in refluxing MeOH (40 ml) for 4 h. Purification of the residue after removal of solvent (TLC; silica gel, acetone/hexane 3:7) gave three bands. The first contained $[\text{RuCl}(\text{PPh}_3)_2\text{Cp}]$ and other unidentified complex **9** (33 mg, 67%). A bright yellow band (R_f 0.42) afforded yellow crystals (benzene/pentane) of $[\text{Ru}_3(\mu\text{-H})(\mu_3\text{-C}_2\text{H})(\mu\text{-dppm})(\text{CO})_6(\text{PPh}_3)]$ (**11**; 15 mg, 23%). IR: see *Table 1*. $^1\text{H-NMR}$: see *Table 1*. ES-MS: see *Table 1*. Analysis: see *Table 1*.

Structure Determinations. For **2**, **4**, and **7**, unique single counter/four-circle diffractometer data sets were measured at ca. 295 K within the specified $2\theta_{\text{max}}$ limits, yielding N independent reflections, N_o with $I > 3\sigma(I)$ considered ‘observed’ and used in the full-matrix least-squares refinements after Gaussian absorption correction. For the remainder, full spheres of data were measured to $2\theta_{\text{max}} = 58^\circ$ with a Bruker AXS-CCD area-detector instrument at the specified temperature, N_{total} reflections being merged to N unique (R_{int} quoted) after ‘empirical’ (multiscan) absorption corrections (proprietary software). N_o Data with $F > 4\sigma(F)$ were used in the refinements. All data were measured with monochromatic MoK_α radiation, $\lambda = 0.71073 \text{ \AA}$. Anisotropic thermal parameter forms were refined for the non-H-atoms, ($x, y, z, U_{\text{iso}})_\text{H}$ included constrained at estimated values. Conventional residuals R, R_w (statistical weights) on $|F|$ are quoted. Neutral atom-complex scattering factors were used; computation used the XTAL 3.7 program system [17]. Pertinent results are given below and in the *Figs.* (which show non-H-atoms with 20% probability amplitude displacement ellipsoids at r.t., or 50% at low temp.; H-atoms have an arbitrary radius of 0.1 Å) and *Tables*. Crystal and refinement data being given in *Table 4*, individual variations associated with each determination, difficulties, etc. being given below.

Complex 2. The available material was badly twinned, the resulting data being refined with a separate scale factor for $0kl$; suitable material was exhausted prior to the availability of the CCD facility. A subsequent crystallisation from benzene yielded a sesquisolvate phase, **2s**, for which ($x, y, z, U_{\text{iso}})_\text{H}$ were refined throughout (CCD data).

Complex 3. Isomorphous benzene and toluene solvates, **3a** and **3b**, resp., were determined with the CCD instrument at ca. 153 K. For **3a**, ($x, y, z, U_{\text{iso}})_\text{H}$ were refined throughout except for the solvent where higher ‘thermal motion’ was evident. For **3b**, ($x, y, z, U_{\text{iso}})_\text{H}$ were constrained at estimated values throughout; for both solvents only small weakly diffracting specimens were available.

Complex 4. Both unsolvated and hexane monosolvate, **4s**, forms were determined. For the former, the PCHP hydrogen complement was assigned on the basis of difference-map residues, refinement behaviour, and associated geometry; material was exhausted prior to the availability of the CCD facility. For the hexane solvate, ($x, y, z, U_{\text{iso}})_\text{H}$ were refined for all components in the structure, the obstreperously disordered solvent molecule excepted. The compound is isomorphous/isostructural with the unsolvated parent, the very considerable increase in cell volume being achieved by the insertion of layers of solvent molecules at $z = 0$ (etc.), the same cell and coordinate setting otherwise being employed (see below).

Complex 7. ($x, y, z, U_{\text{iso}})_\text{H}$ were refined for the core H-atoms; Ph ring 22 was modelled as disordered over two sets of sites, occupancies refining to 0.60(1) and complement. In the solvate **7s**, difference map residues were modelled as CH_2Cl_2 of solvation, totalling a hemisolvate, disposed on a crystallographic 2-axis, C isotropic. ($x, y, z, U_{\text{iso}})_\text{H}$ were refined throughout except for those associated with the solvent where ‘thermal motion’ was high.

Complex 9s. Considerable disorder was encountered among the Ph rings of the dppm ligands, rings 11, 22, 32, and 42 each being modelled as disposed over two sets of sites, with occupancies of major and minor components seemingly concerted, set with common populations refining to 0.773(5) and complement after trial

Table 4. Crystal Data and Refinement Details

Compound	2	2s	3a	3b	4
Formula	C ₃₇ H ₂₈ O ₆ P ₂ Ru ₃	C ₃₇ H ₂₈ O ₆ P ₂ Ru ₃ · 1.5 C ₆ H ₆	C ₃₇ H ₂₈ O ₆ P ₂ Ru ₃ · C ₆ H ₆	C ₃₇ H ₂₈ O ₆ P ₂ Ru ₃ · C ₇ H ₈	C ₄₀ H ₃₀ O ₇ P ₂ Ru ₃
<i>T</i> /K	ca. 295	ca. 153	ca. 153	ca. 153	ca. 295
Mol.-wt.	933.8	1051.0	1011.9	1025.9	978.8
Crystal system	Monoclinic	Monoclinic	Monoclinic	Monoclinic	Orthorhombic
Space group	<i>P</i> ₂ ₁ / <i>c</i> (#14)	<i>P</i> ₂ ₁ / <i>n</i> (#14)	<i>P</i> ₂ ₁ / <i>c</i> (#14)	<i>P</i> ₂ ₁ / <i>c</i> (#14)	<i>Pbca</i> (#16)
<i>a</i> /Å	16.219(6)	12.618(2)	9.6290(9)	9.665(1)	16.633(3)
<i>b</i> /Å	10.925(4)	24.877(3)	20.283(2)	20.644(2)	17.334(10)
<i>c</i> /Å	24.976(16)	13.731(2)	21.198(2)	21.433(2)	27.292(4)
<i>α</i> /deg.					
<i>β</i> /deg.	127.78(4)	101.835(2)	110.822(2)	111.272(2)	
<i>γ</i> /deg.					
<i>V</i> /Å ³	3498	4219	3970	3985	7869
<i>Z</i>	4	4	4	4	8
<i>D</i> _x /g cm ⁻³	1.77 ₄	1.65 ₅	1.73 ₇	1.71 ₁	1.66 ₇
<i>μ</i> /cm ⁻¹	14.2	11.8	12.9	12.5	12.7
Crystal size/mm	0.10 × 0.32 × 0.25	0.35 × 0.18 × 0.09	0.32 × 0.11 × 0.04	0.12 × 0.07 × 0.04	0.42 × 0.65 × 0.10
<i>T</i> _{min,max}	0.72, 0.86	0.65, 0.86	0.74, 0.89	0.77, 0.89	0.63, 0.84
2 <i>θ</i> _{max} /deg.	45	58	58	50	55
<i>N</i> _{tot}		42173	38974	31157	
<i>N</i> _i (<i>R</i> _{int})	6085	10701 (0.041)	9925 (0.054)	7079 (0.072)	6946
<i>N</i> _o	3200	8722	7016	4443	3619
<i>R</i>	0.073	0.033	0.039	0.042	0.058
<i>R</i> _w	0.081	0.042	0.039	0.040	0.059
<i>Δρ</i> _{max} /e Å ³	1.68(4)	1.00(7)	1.2(1)	0.9(1)	1.1(1)
Compound	4s	7	7s	9s	11s
Formula	C ₄₀ H ₃₀ O ₇ P ₂ Ru ₃ · C ₆ H ₁₄	C ₃₅ H ₂₄ O ₇ P ₂ Ru ₃	C ₃₅ H ₂₄ O ₈ P ₂ Ru ₃ · 0.5 CH ₂ Cl ₂	C ₆₆ H ₄₈ O ₁₂ P ₄ Ru ₆ · 3 C ₆ H ₆	C ₃₇ H ₄₅ O ₆ P ₃ Ru ₃ · C ₆ H ₆
<i>T</i> /K	ca. 153	ca. 295	ca. 300	ca. 300	ca. 300
Mol.-wt.	1074.0	937.7	980.2	1997.8	1222.1
Crystal system	Orthorhombic	Monoclinic	Monoclinic	Monoclinic	Monoclinic
Space group	<i>Pbca</i> (#61)	<i>P</i> ₂ ₁ / <i>c</i> (#14)	<i>C</i> ₂ / <i>c</i> (#15)	<i>P</i> ₂ ₁ / <i>c</i> (#14)	<i>P</i> ₂ ₁ (#4)
<i>a</i> /Å	16.406(1)	14.892(3)	33.287(7)	16.139(1)	13.015(1)
<i>b</i> /Å	17.428(1)	12.374(7)	12.297(3)	20.264(1)	15.623(1)
<i>c</i> /Å	30.652(2)	22.536(3)	24.158(5)	24.894(2)	13.670(1)
<i>α</i> /deg.					
<i>β</i> /deg.		122.39(1)	131.427(3)	96.915(1)	106.590(1)
<i>γ</i> /deg.					
<i>V</i> /Å ³	8854	3492	7415	8082	2664
<i>Z</i>	8	4	8	4	2
<i>D</i> _x /g cm ⁻³	1.61 ₁	1.78 ₃	1.75 ₆	1.64 ₂	1.52 ₁
<i>μ</i> /cm ⁻¹	11.3	14.2	14.1	12.3	9.8
Crystal size/mm	0.17 × 0.14 × 0.06	0.14 × 0.28 × 0.22	0.15 × 0.12 × 0.10	Cuboid, ca. 0.2	0.20 × 0.20 × 0.05
<i>T</i> _{min,max}	0.68, 0.89	0.70, 0.84	0.66, 0.91	0.64, 0.93	0.60, 0.83
2 <i>θ</i> _{max} /deg.	58	55	58	58	58
<i>N</i> _{tot}	87034		39476	89637	29818
<i>N</i> _i (<i>R</i> _{int})	11570 (0.067)	8001	9384 (0.048)	20561 (0.092)	7059 (0.053)
<i>N</i> _o	8989	5424	5131	9865	5367
<i>R</i>	0.061	0.037	0.048	0.051	0.044
<i>R</i> _w	0.073	0.037	0.046	0.050	0.054
<i>Δρ</i> _{max} /e Å ³	4.0(1)	0.6	1.7(1)	1.07(9)	0.86(7)

refinement. Three independent residues modelled as benzene solvent were found, all with high displacement amplitudes but no resolvable disorder, residues 2,3 being modelled as rigid bodies and site occupancies set at unity after trial refinement.

Complex 11s. A large void about the crystallographic *b* axis is occupied by residues modelled as a single benzene of solvation, propagated up the void by the 2₁ screw. Although disorder was not resolved, displacement parameters were very high, and the molecule was ultimately modelled as a rigid-body, site occupancy set at unity after trial refinement. In the circumstances, the core H-atom could not be satisfactorily located and is postulated on the basis of the chemistry. ‘Friedel pair’ data were retained distinct, ‘*x*_{abs}’ refining to –0.08(7).

We thank the *Australian Research Council* for support of this work and *Johnson Matthey plc*, Reading, for a generous loan of $\text{RuCl}_3 \cdot n \text{H}_2\text{O}$.

References

- [1] a) E. Sappa, A. Tiripicchio, P. Braunstein, *Chem. Rev.* **1983**, *83*, 203; b) P. R. Raithby, M. J. Rosales, *Adv. Inorg. Chem. Radiochem.* **1985**, *29*, 169; c) A. J. Deeming, A. J. Arce, Y. De Sanctis, *Mater. Chem. Phys.* **1991**, *29*, 323; d) E. Sappa, *J. Cluster Sci.* **1994**, *5*, 211; e) M. Akita, Y. Moro-oka, *Bull. Chem. Soc. Jpn.* **1995**, *68*, 420; f) S. Deabate, R. Giordano, E. Sappa, *J. Cluster Sci.* **1997**, *8*, 407; g) M. J. Morris, in 'Metal Clusters in Chemistry', Eds. P. Braunstein, L. A. Oro, and P. R. Raithby, Wiley-VCH, Weinheim, 1999, Chapt. 1.13, p. 221; h) A. A. Koridze, *Russ. Chem. Bull.* **2000**, *49*, 1.
- [2] a) M. I. Bruce, B. W. Skelton, A. H. White, N. N. Zaitseva, *J. Chem. Soc., Dalton Trans.* **1999**, 1445; b) M. I. Bruce, B. W. Skelton, A. H. White, N. N. Zaitseva, *Aust. J. Chem.* **1999**, *52*, 413; c) M. I. Bruce, B. W. Skelton, A. H. White, N. N. Zaitseva, *Aust. J. Chem.* **1999**, *52*, 681.
- [3] M. I. Bruce, B. W. Skelton, A. H. White, N. N. Zaitseva, *J. Chem. Soc., Dalton Trans.* **1999**, 13.
- [4] M. I. Bruce, N. N. Zaitseva, B. W. Skelton, A. H. White, *J. Chem. Soc., Dalton Trans.* **1999**, 2777.
- [5] a) A. J. Deeming, in 'Comprehensive Organometallic Chemistry II', Eds. E. W. Abel, F. G. A. Stone, and G. Wilkinson, Elsevier, Oxford, 1995, Vol. 7, Chapt. 12, p. 683; b) M. I. Bruce, P. A. Humphrey, H. Miyamae, B. W. Skelton, A. H. White, *J. Organomet. Chem.* **1992**, *429*, 187; c) M. I. Bruce, P. A. Humphrey, E. Horn, E. R. T. Tiekink, B. W. Skelton, A. H. White, *J. Organomet. Chem.* **1992**, *429*, 207; d) M. I. Bruce, J. R. Hinchliffe, P. A. Humphrey, R. J. Surynt, B. W. Skelton, A. H. White, *J. Organomet. Chem.* **1998**, *552*, 109.
- [6] A. B. Holmes, C. L. D. Jennings-White, A. H. Schulthess, B. Kinde, D. R. M. Walton, *J. Chem. Soc., Chem. Commun.* **1979**, 840.
- [7] M. I. Bruce, B. C. Hall, B. D. Kelly, P. J. Low, B. W. Skelton, A. H. White, *J. Chem. Soc., Dalton Trans.* **1999**, 3179.
- [8] J. R. Bleeke, R. Behm, Y.-F. Xie, M. Y. Chiang, K. D. Robinson, A. M. Beatty, *Organometallics* **1997**, *16*, 606.
- [9] A. J. Carty, S. A. MacLaughlin, N. J. Taylor, *J. Chem. Soc., Chem. Commun.* **1981**, 476.
- [10] R. D. Adams, X. Qu, W. Wu, *Organometallics* **1994**, *13*, 1272.
- [11] G. Predieri, A. Tiripicchio, C. Vignali, E. Sappa, *J. Organomet. Chem.* **1988**, *342*, C33.
- [12] C. J. Adams, M. I. Bruce, P. A. Duckworth, P. A. Humphrey, O. Kühl, E. R. T. Tiekink, W. R. Cullen, P. Braunstein, S. C. Cea, B. W. Skelton, A. H. White, *J. Organomet. Chem.* **1994**, *467*, 251.
- [13] a) M. I. Bruce, A. G. Swincer, *Adv. Organomet. Chem.* **1983**, *22*, 59; b) M. I. Bruce, *Chem. Rev.* **1991**, *91*, 197.
- [14] K. Henrick, M. McPartlin, A. J. Deeming, S. Hasso, P. J. Manning, *J. Chem. Soc., Dalton Trans.* **1982**, 899.
- [15] Y. Chi, A. J. Carty, P. Blenkiron, E. Delgado, G. D. Enright, W. Wang, S.-M. Peng, G. H. Lee, *Organometallics* **1996**, *15*, 5269.
- [16] M. I. Bruce, B. K. Nicholson, M. L. Williams, *Inorg. Synth.* **1989**, *26*, 276.
- [17] The XTAL 3.7 System, Eds. S. R. Hall, D. J. du Boulay, R. Olthof-Hazekamp, University of Western Australia, 2000.

Received 12 June 2001